

# COMPARISON OF PREDICTED AND MEASURED AEROSOL OPTICAL AND PHYSICAL PROPERTIES IN AUSTRALIAN CITIES

Yoshiteru Iinuma<sup>1</sup>, Gail P. Box<sup>1</sup>, John L. Gras<sup>2</sup>, Melita Keywood<sup>2</sup> and Gregory Ayers<sup>2</sup>

<sup>1</sup>Atmospheric Group, School of Physics, The University of New South Wales, Sydney, NSW 2052, Australia

<sup>2</sup>CSIRO Atmospheric Research, PMB 1, Aspendale, Vic 3195, Australia

## Summary

Comprehensive information on the optical and physical properties of aerosol particles is important for evaluating or estimating the effects of aerosol on air quality, visibility degradation and radiative forcing. The determination of extinction of light by ambient aerosol particles can be achieved successfully by the accurate estimation of aerosol refractive index using observed and modelled size-resolved chemical composition data. Physical and chemical properties of the aerosol in major Australian cities were measured by various instruments during a field campaign in 1997, which included a PMS ASASP-X aerosol spectrometer, nephelometers, a MOUDI multistage impactor and a TEOM mass balance. Our work employs a thermodynamic equilibrium model for the prediction of aerosol chemical properties and density, a partial molar refraction approach for mean aerosol refractive index and Mie calculation for the prediction of scattering coefficients. This paper presents the results from our model and comparison with data obtained during the study.

*Keywords:* Atmospheric Aerosols, Refractive Index, Density, Thermodynamic Model, SCAPE2, Partial Refraction Approach

## 1. Introduction

Atmospheric aerosols play an important role in air quality, visibility and radiative forcing in the atmosphere. The chemical composition of aerosol varies spatially and temporally, and it is a highly complex mixture. Atmospheric aerosols are generally composed of water soluble inorganic salts, organic species, elemental carbon, trace elements and water. Inorganic salts are known to be hygroscopic by nature, and recent emphasis is on estimation of the effects on optical properties of aerosol due to hygroscopicity using a thermodynamic model (e.g., Tang, 1996, 1997; Malm *et al.*, 1997; Sloane, 1984; Tang and Munkelwitz, 1994; Koloutsou-Vakakis and Rood, 1998). Aerosol particles will take up water as relative humidity (RH) increases thus altering the particle size distribution, the composition of the particles and their refractive index. When RH decreases, water evaporates and consequently, scattering coefficient,  $b_{\text{scat}}$ , changes.

In the past, a number of studies have investigated humidity-dependent water uptake by aerosols, theoretically or empirically, with various degrees of success. Theoretical estimation of water uptake by aerosols has improved significantly with the recent development of thermodynamic models such as SCAPE and SCAPE2 (Kim *et al.*, 1993 a,b; Kim and Seinfeld, 1995; Meng *et al.*, 1995), MARS-A (Binkowski and Shankar, 1995), EQUISOLV II (Jacobson, 1999), and AIM2 (Clegg *et al.*, 1998a,b). Still there are many

problems to be addressed such as a lack of thermodynamic data available for the calculations, especially for organic species.

Models need to be verified with measurements and *vice versa*. This feedback loop will identify how well measured parameters can be predicted given restrictions in terms of data acquired. It is a necessary step towards the understanding of observed physical process and more accurate prediction.

The objective of this paper is to estimate of  $b_{\text{scat}}$ , humidity growth and other physical parameters of the ambient aerosol based on field measurements of chemical and physical properties of Australian fine particles (AFP study). The modelling procedures are also described, and the results are compared with measurements.

## 2. Modelling

The aim of modelling in this study is to estimate  $b_{\text{scat}}$  as a function of relative humidity, size distribution, and composition. The first step is to characterise the chemistry of the ambient aerosol as a function of RH using a thermodynamic model. The second step is to calculate optical properties of ambient aerosol using the partial molar refraction approach (Stelson, 1990) and MIE theory and utilising the chemistry data obtained from the first step.

## 2.1. Estimation of Aerosol Composition

SCAPE2 (Kim and Seinfeld, 1995; Meng *et al.*, 1995) is used in this study to predict the physical and molecular state of atmospheric aerosol at thermodynamic equilibrium. Input parameters for SCAPE2 are  $[\text{Na}^+]$ ,  $[\text{SO}_4^{2-}]$ ,  $[\text{NH}_4^+]$ ,  $[\text{NO}_3^-]$ ,  $[\text{Cl}^-]$ ,  $[\text{K}^+]$ ,  $[\text{Ca}^{2+}]$ ,  $[\text{Mg}^{2+}]$ ,  $[\text{CO}_3^{2-}]$ , RH and T. The concentration of  $\text{H}_2\text{CO}_3$  was obtained from an annual average  $\text{CO}_2$  of 356.2 ppm at Cape Grim in 1994 (Steele *et al.*, 1996). RH of 20% and 80% are assumed for dry and ambient aerosols respectively. Temperature is assumed to be 293K. The inverted size resolved chemical mass concentration data (described in 4.4) were amalgamated from 72 size bins to 12 size bins by taking geometric means. The thermodynamic equilibrium calculation was carried out for each size bin for both dry and ambient aerosols. The output species from SCAPE2 are  $(\text{NH}_4)_2\text{SO}_4$ ,  $(\text{NH}_4)_3\text{H}(\text{SO}_4)_2$ ,  $\text{H}_2\text{CO}_3$ ,  $\text{H}_2\text{SO}_4$ ,  $\text{Ca}(\text{HCO}_3)_2$ ,  $\text{Ca}(\text{NO}_3)_2$ ,  $\text{CaCl}_2$ ,  $\text{CaCO}_3$ ,  $\text{CaSO}_4$ ,  $\text{HCl}$ ,  $\text{HNO}_3$ ,  $\text{K}_2\text{CO}_3$ ,  $\text{K}_2\text{SO}_4$ ,  $\text{KCl}$ ,  $\text{KHCO}_3$ ,  $\text{KHSO}_4$ ,  $\text{KNO}_3$ ,  $\text{Mg}(\text{HCO}_3)_2$ ,  $\text{Mg}(\text{NO}_3)_2$ ,  $\text{MgCl}_2$ ,  $\text{MgCO}_3$ ,  $\text{MgSO}_4$ ,  $\text{Na}_2\text{CO}_3$ ,  $\text{Na}_2\text{SO}_4$ ,  $\text{NaCl}$ ,  $\text{NaHCO}_3$ ,  $\text{NaHSO}_4$ ,  $\text{NaNO}_3$ ,  $(\text{NH}_4)_2\text{CO}_3$ ,  $\text{NH}_4\text{Cl}$ ,  $\text{NH}_4\text{HCO}_3$ ,  $\text{NH}_4\text{HSO}_4$ ,  $\text{NH}_4\text{NO}_3$ , and water. Elemental carbon (EC) concentration was determined by light absorption at the wavelength of 565 nm using the integrated plate method (Lin *et al.*, 1973). Organic mass is assumed to be the following:

$$[\text{Organic Mass}] = [\text{Gravimetric Mass}] - [\text{Inorganic Mass}] - [\text{Elemental Carbon}]. \quad (1)$$

Considerable efforts are being made by many scientists to improve understanding of the physical and chemical properties of organic aerosol. However, these properties are still poorly understood. In the AFP study, the organic aerosol fraction was not characterised, so published values of the density and refractive index of organic aerosol are used (Larson *et al.*, 1988). Both EC and organic species are presumed to be non-hygroscopic in this study.

## 2.2. Estimation of Refractive Index and Density

The refractive index and density of ambient aerosol depend on the chemical composition as well as RH. The refractive index is estimated for each size bin for both dry and ambient aerosol by using the partial molar refraction approach (Stelson, 1990). The mean aerosol density for both dry and ambient aerosols are estimated as the concentration-weighted average for each size bin (Stelson, 1990). RI and densities for various species are obtained from the literature and published data (Stelson, 1990; Larson *et al.*, 1988; Lide, 1997-1998; Washburn, 1926).

## 2.3. Estimation of Optical Properties

The scattering efficiency,  $Q_{\text{scat}}$ , is calculated using a MIE program from Bohren and Huffman (1983) for each size bin at a wavelength of 530 nm to emulate nephelometer measurements. Scattering coefficient,  $b_{\text{scat}}$ , is obtained

Table 1. Sampling locations, period and number of samples

Sampling Location	Sampling Period	No. of Samples
Adelaide, Therbaton	1/8/97-27/8/97	5
Brisbane, Rocklea	25/9/96-24/11/96	5
Canberra, Monash	3/5/97-4/6/97	3
Launceston, Ti Tree Bend	10/6/97-25/7/97	6
Melbourne, Footscray	3/4/97-27/4/97	5
Sydney, Liverpool	20/8/96-15/9/96	4

by integrating Qscat over the number size distribution,  $dN/d\log D$ .

## 3. Sampling and Analysis

### 3.1. Sampling Site and Date

Samples were collected as a part of a study of the chemical and physical properties of Australian fine particles (AFP Study) between July 1996 and August 1997. Aerosol chemistry data were collected over 24 hour periods during about four weeks in each city. Sampling locations, period and the number of samples are listed in Table 1.

### 3.2. Sampling System

The chemistry samples were collected by a 12-stage MOUDI (Micro-Orifice Uniform Deposit Impactor) with polycarbonate Poretics filters, 0.47  $\mu\text{m}$  pore size and 47 mm in diameter, for the first 11 stages (Inlet to stage 10) and a teflon-backed Fluoropore filter, 1  $\mu\text{m}$  pore size and 37 mm in diameter for the back-up stage.

Aerosol scattering coefficients were measured at a wavelength of 530 nm with Radiance Research type M903 nephelometers. Two nephelometers were operated at the same time to determine dry and (near) ambient scattering coefficients. Both nephelometers were calibrated using the refrigerant gas R22 and filtered air, normally once a sampling period.

In order to test a validity of MOUDI derived size distributions, aerosol size distributions were obtained using a Particle Measuring Systems Inc. ASASP-X (Active-cavity-laser Particle Size Spectrometer), which measures the particle size range from 0.1  $\mu\text{m}$  to 3  $\mu\text{m}$  into 60 size bins in four overlapping size ranges. The instrument was calibrated using monodisperse polystyrene latex particles at the beginning and end of each sampling period.

### 4.4. Analysis

MOUDI filters were weighed to determine gravimetric mass using a Mettler MT5 microbalance at a relative humidity of less than 20%. The concentrations of soluble inorganic species were determined by Dionex DX500 suppressed ion chromatography.

Chemical mass concentrations obtained from the MOUDI filters were inverted using an efficient, non-linear iterative inversion procedure (Twomey &

	nssK	Br	Pb	Organics	EC	Mass $\mu\text{g}/\text{m}^3$
Launceston	0.70	0.04	0.11	71.16	4.87	181
Canberra	0.56	0.06	0.22	78.03	8.30	153
Adelaide	0.18	0.29	0.82	59.81	10.48	93
Brisbane	1.15	0.02	0.10	46.59	6.19	95
Melbourne	0.15	0.02	0.11	68.26	2.42	100
Sydney	0.49	0.03	0.42	67.87	9.55	103

Zabalsky, 1981; Winklmayr *et al.*, 1990) to obtain a smooth size distribution.

## 4. Results

### 4.1. Characteristics of Aerosols

Two distinct types of aerosol were observed.

- Winter time aerosol, which is dominated by emissions from domestic wood burning. This type of aerosol was characterised by high particle loadings, high concentrations of organic species and nssK<sup>+</sup>, and a relatively low concentration of EC.
- Urban aerosol, which has a greater contribution from automobile emissions. This type of aerosol was characterised by high concentration of Br, Pb and EC.

Canberra and Launceston aerosols were dominated by the emission from domestic wood burning; the other cities were mainly dominated by urban aerosols (Table 2).

### 4.2. Density and Refractive Index

A density minimum is predicted between 0.1-1.0  $\mu\text{m}$  diameter, corresponding to the presence of organics. For refractive index, a peak is predicted around 0.1  $\mu\text{m}$  diameter for both real and imaginary parts. This coincides with high EC concentration in this size range. Some examples of density and refractive index as a function of geometric diameter in Canberra are shown in Figures 1 and 2. The effect of hygroscopicity on density and refractive index can be seen in both figures with lower density and real part of the refractive index, and higher imaginary part of the refractive index for 80% relative humidity.

### 4.3. Size Distributions

Size distribution,  $\text{dN}/\text{dlogD}$ , is estimated from gravimetric mass, water mass, geometric diameter and density for both dry and ambient aerosol. An example of estimated  $\text{dN}/\text{dlogD}$  and an ASASP-X measurement comparison is shown in Figure 3. ASASP-X and predicted  $\text{dN}/\text{dlogD}$  agree well although the predicted size distribution shows slight overestimation at larger than 1.0  $\mu\text{m}$  diameter.

Overall, the size distributions from all the cities exhibit similar patterns, although it is evident that the Canberra and Launceston aerosol had much higher

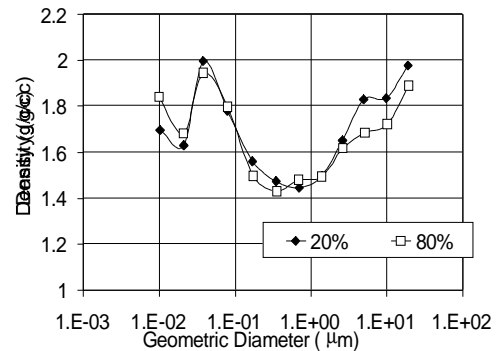


Figure 1. Density as a function of geometric diameter for Canberra 3 June 1997.

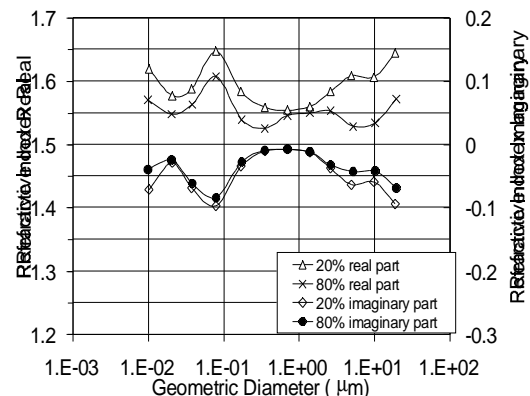


Figure 2. Refractive index as a function of geometric diameter for Canberra 3 June 1997.

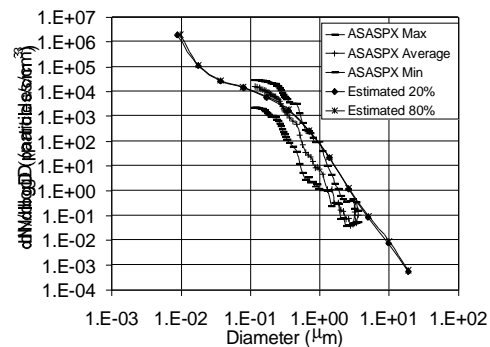


Figure 3. Estimated  $\text{dN}/\text{dlogD}$  and ASASP-X for Canberra 3 June 1997

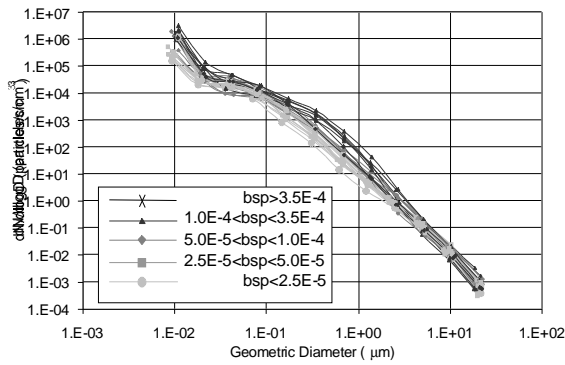


Figure 4. Predicted size distribution as a function of geometric diameter at RH 20%. Plots are classified into 5 categories by  $b_{scat}$  value

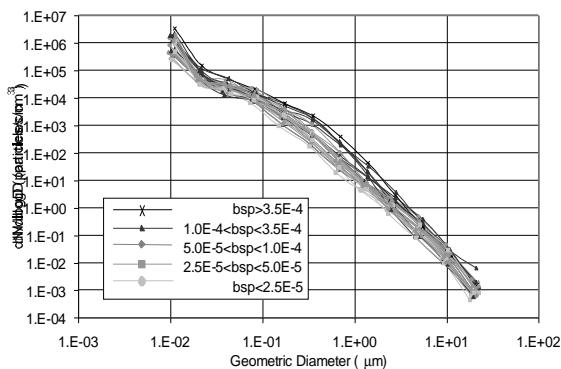


Figure 5. Predicted size distribution as a function of geometric diameter at RH 80%. Plots are classified into 5 categories by  $b_{scat}$  value

particle loadings than other cities, due to domestic wood burning. Mode diameters were observed around  $0.02 \mu\text{m}$  and  $0.3 \mu\text{m}$ . Size distributions from all sampling locations are shown in Figure 4 and 5 for RH at 20% and 80% respectively. In Adelaide, Brisbane, Melbourne, and Sydney scattering coefficients were typically lower than  $5 \times 10^{-5} \text{ m}^{-1}$  and the characteristics of chemical composition were typically dominated by automobile emissions. On the other hand, Launceston and Canberra aerosols had much higher scattering coefficients and the chemical composition shows that domestic wood burning smoke is the dominant aerosol source. Size distributions from samples with smaller particle mass and organic species contributions (i.e. Adelaide, Brisbane, Melbourne, and Sydney) show more apparent hygroscopic growth in both the fine and coarse modes compared to domestic wood burning aerosols (i.e. Launceston and Canberra).

#### 4.5. Differential Scatter Distributions

The differential scatter distributions are shown in Figures 6 and 7 for RH at 20% and 80% respectively. Differential scatter distributions show that light scattering is dominated by particles with a diameter between  $0.3 - 1.0 \mu\text{m}$ , with a peak scattering efficiency

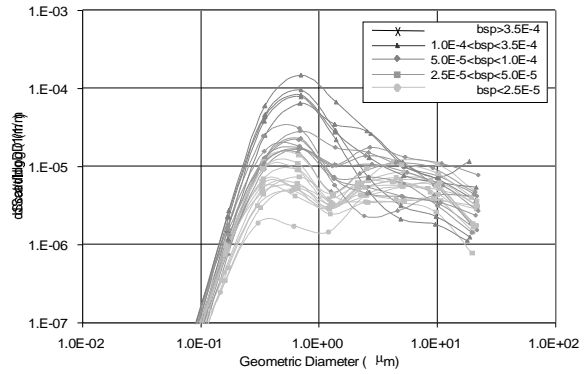


Figure 6. Predicted differential scatter as a function of geometric diameter at RH 20%. Plots are classified into 5 categories by  $b_{scat}$  value

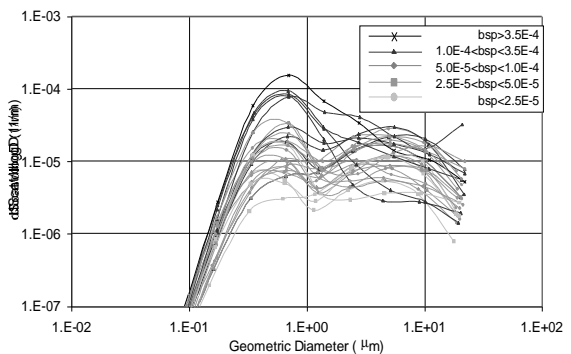


Figure 7. Predicted differential scatter as a function of geometric diameter at RH 80%. Plots are classified into 5 categories by  $b_{scat}$  value

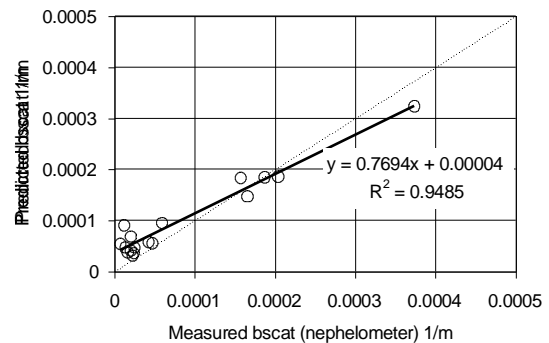


Figure 8. Comparison of measured  $b_{scat}$  and modelled  $b_{scat}$  for Adelaide, Canberra, Launceston and Melbourne at RH 20%. No comparable nephelometer data were available for Brisbane and Sydney.

around  $0.3 - 0.7 \mu\text{m}$  (at wavelength of  $530 \text{ nm}$ ). At low mass loadings and scattering levels such as Brisbane there is a relatively high contribution from large particles but this is not so apparent for the cases of high mass loadings and scattering levels. The effect of RH on  $dScat/dlogD$  is much more apparent for larger particle sizes than smaller particle sizes with an elevated peak between  $1 - 10 \mu\text{m}$  (Figure 7).

## 4.6. Comparison to Nephelometer

Comparison between measured  $b_{\text{scat}}$  from the nephelometer and modelled  $b_{\text{scat}}$  at RH 20% is shown in Figure 8. Coincident nephelometer and MOUDI data sets are only available for Adelaide, Canberra, Launceston and Melbourne. The agreement between measured  $b_{\text{scat}}$  and modelled  $b_{\text{scat}}$  is reasonably good although the model has a tendency to predict larger  $b_{\text{scat}}$  than the nephelometer for low mass loading samples and smaller  $b_{\text{scat}}$  for very high mass loading samples.

The discrepancy between the two may be attributed to (1) the shape of aerosol particles, (2) difference in refractive index used for the model and instrument for calibration, (3) modelled hygroscopic growth and “real” hygroscopic growth and (4) assumptions made about organic species and EC.

## 5. Conclusion

This study presents a potentially useful method for deriving the optical, physical and chemical properties of atmospheric aerosols. Measured and modelled light scattering show reasonable agreement although the model over-predicts  $b_{\text{scat}}$  for low mass loading samples and under-predicts for high mass loading samples. In order to reduce uncertainty of the predicted optical properties of atmospheric aerosols, properties of organic species and EC such as refractive index and hygroscopicity need to be assessed in detail.

## Acknowledgments & Disclaimer

We wish to thank Environment Australia for funding the Fine Particle Study. We also thank the ACT government Analytical Laboratories for their assistance and Dr. Pradeep Saxena for providing us SCAPE2.

The views expressed are not necessarily the views of the Commonwealth of Australia, or State Authorities, and the Commonwealth of Australia or State Authorities do not accept responsibility in any information or advice given in relation to, or as a consequence of, anything contained herein.

## References

Binkowski, F.S. and Shankar, U., 1995, ‘The regional particulate matter model. 1: model description and preliminary results’, *Journal of Geophysical Research*, **100**:26,191-26,209

Bohren, C.F. and Huffman, D.R., 1983, ‘Absorption and scattering of light by small particles’, Wiley, New York.

Clegg S.L., Brimblecomb, P., Wexler A.S., 1998a, ‘A thermodynamic model of the system  $\text{H}^+\text{-NH}_4^+\text{-Na}^+\text{-SO}_4^{2-}\text{-NO}_3^-\text{-Cl}^-\text{-H}_2\text{O}$  at 298.15K’, *Journal of Physical Chemistry*, **102**:2155-2171

Clegg S.L., Brimblecomb, P., Wexler A.S., 1998b, ‘A thermodynamic model of the system  $\text{H}^+\text{-NH}_4^+\text{-Na}^+\text{-SO}_4^{2-}\text{-NO}_3^-\text{-Cl}^-\text{-H}_2\text{O}$  at tropospheric temperature’, *Journal of Physical Chemistry*, **102**:2137-2154

Jacobson, M.Z. 1999, ‘Studying the effects of calcium and magnesium on size distributed nitrate and ammonium with EQUISOLV II’, *Atmospheric Environment*, **33**:3635-3649

Kim, Y. P., Seinfeld, J. H. & Saxena, P. 1993a, ‘Atmospheric gas-aerosol equilibrium I. thermodynamic model’, *Aerosol Science & Technology*, **19**:157-181

Kim, Y. P., Seinfeld, J. H. & Saxena, P. 1993b, ‘Atmospheric gas-aerosol equilibrium II. analysis of common approximation and activity coefficient calculation methods’, *Aerosol Science & Technology*, **19**:182-198

Kim, Y. P. and Seinfeld, J. H. 1995, ‘Atmospheric gas-aerosol equilibrium III. thermodynamics of crustal elements  $\text{Ca}^{2+}$ ,  $\text{K}^+$ ,  $\text{Mg}^{2+}$ ’, *Aerosol Science & Technology*, **22**:93-110

Koloutsou-Vakakis S. and Rood M.J., 1998, ‘Modeling of aerosol properties related to direct climate forcing’, *Journal of Geophysical Research*, **103**: 17,009-17,032

Larson S. M., Cass, G. R., Hussey, K. J. & Luce, F. 1988, ‘Verification of Image Processing Based Visibility Models’, *Environmental Science Technology*, **22**:629-637

Lide (ed.) 1997-1998, CRC handbook of chemistry, 78th ed.

Lin C. I., Baker M., Charlson R. C. 1973, ‘Absorption coefficient of atmospheric particles’, *Applied Optics*, **12**:1357-1363.

Malm W.C. and Kreidenweis S.M., 1997, ‘The effects of models of aerosol hygroscopicity on the apportionment of extinction’, *Atmospheric Environment*, **31**:1965-1976

Meng, Z., Saxena, P. & Kim, Y. P. 1995, ‘Atmospheric gas-aerosol equilibrium IV. thermodynamics of carbonates’, *Aerosol Science & Technology*, **23**:131-154

Sloane C.S., 1984 ‘Optical properties of aerosols of mixed composition’, *Atmospheric Environment*, Vol. **18**:871-878

Steele, L. P., Beardsmore, D. J., Pearman, G. I. & Da Costa, G. A., ‘Baseline carbon dioxide monitoring’, *Baseline Atmospheric Program Australia 1994-95*, Bureau of Meteorology and CSIRO DAR, pp.103

Stelson A. W. 1990, ‘Urban aerosol refractive index prediction by partial molar refraction approach’, *Environmental Science and Technology*, **24**:1676-1679

Tang I.N., 1996, ‘The effects of models of aerosol hygroscopicity on the apportionment of extinction’, *Journal of Geophysical Research*, **101**:19,245-19,250

Tang I.N., 1997, ‘Thermodynamic and optical properties of mixed-salt aerosols of atmospheric importance’, *Journal of Geophysical Research*, **102**:1883-1893

Tang I.N. and Munkelwitz H.R., 1994, ‘Water activities, densities, and refractive indices of aqueous sulfates and sodium nitrate droplets of atmospheric importance’, *Journal of Geophysical Research*, **99**: 18,801-18,808

- Twomey S. A. and Zalabsky R. A. 1981, 'Multifilter technique for examination of the size distribution of the natural aerosol in the submicrometer range', *Environmental Science and Technology*, **15**:177-184.
- Washburn (ed.) 1926 International Critical Tables of Numerical Data; Physics Chemistry and Technology, Volume 1
- Winklmayr W., Wang H-C. & John W. 1990, 'Adaptation of the Twomey algorithm to the inversion of cascade impactor data', *Aerosol Science and Technology*, **13**:322-331.